Adsorption and deposition of anthraquinone-2-carboxylic acid on alumina studied by inelastic electron tunneling spectroscopy, infrared reflection absorption spectroscopy, X-ray photoelectron spectroscopy, and atomic force microscopy

Morihide Higo [a,*], Takeshi Miake [a,1], Masaru Mitsushio [a],
Toshifumi Yoshidome [a], Yoshihisa Ozono [b]

[a] *Department of Applied Chemistry and Chemical Engineering, Faculty of Engineering, Kagoshima University,*
1-21-40 Korimoto, Kagoshima 890-0065, Japan
[b] *Center for Instrumental analysis, Kagoshima University, 1-21-40 Korimoto, Kagoshima 890-0065, Japan*

Abstract

The adsorption state of anthraquinone-2-carboxylic acid (AQ-2-COOH) deposited from acetone solutions (0.01–1.00 mg/ml) on native oxide surfaces of Al films was characterized by inelastic electron tunneling spectroscopy, infrared reflection absorption spectroscopy, and X-ray photoelectron spectroscopy. The oxide was prepared on evaporated Al films at room temperature in an oxygen-dc glow discharge. The morphology of the deposited AQ-2-COOH on the oxide surfaces was observed and analyzed by atomic force microscopy. These surface analyses showed that AQ-2-COOH is adsorbed predominantly as a uniform nanometer-scale film of carboxylate anions on the oxide surfaces deposited from solutions with concentrations lower than or equal to 0.02 mg/ml. It was found that AQ-2-COOH is adsorbed as both a uniform film of anions and as micron-sized particles of neutral molecules with heights of a few tens of nanometers when AQ-2-COOH is deposited from solutions with concentrations higher than 0.02 mg/ml. A comparison of the results obtained by these surface analytical techniques clearly shows the features and advantages of these analytical techniques.

1. Introduction

Inelastic electron tunneling spectroscopy (IETS) is a unique analytical technique for investigating a thin (nm) insulator film of a metal/insulator/metal (MIM) tunneling junction, providing vibrational information about the insulator at cryogenic temperatures [1–9]. The insulator typically consists of a metal oxide layer with adsorbed species on the surface. The high sensitivity, good resolution, and wide spectral range of IETS enable one to obtain a detailed vibrational spectrum of the adsorbed species on the oxide surface of the metal electrode. Since the dipole and induced dipole moments couple to tunneling electrons, both infrared-active and Raman-active vibrational modes are observed in the IETS spectrum. IETS has an orientational preference: an oscillating dipole moment perpendicular to the oxide surface generally couples to tunneling electrons more strongly than that parallel to the surface. The junction is prepared sequentially by metal evaporation, oxidation, sample adsorption, and top electrode evaporation. Aluminum is widely used as the metal electrode, not only because of the excellent chemical, physical, and electrical stability of the oxide, but also because of its ease of

* Corresponding author. Tel.: +81 99 285 8340; fax: +81 99 285 8344.
E-mail address: higo@apc.kagoshima-u.ac.jp (M. Higo).
[1] Present address: Sony Semiconductor Kyushu Co., 6-33 Tsukuba-machi, Isahaya-shi, Nagasaki 854-0065, Japan.

formation. Lead is used as a good top electrode, because of its relatively low reactivity and large atomic size. Moreover, lead is superconducting at cryogenic temperatures thereby improving the sensitivity and resolution of the IETS spectrum. The tunneling spectra of evaporated thin (nm) films of Si and Ge on the oxides of Al have also been obtained [7,8]. Thus, IETS is a powerful surface analytical technique for investigating oxides and semiconductors, and its application to many fields of science and technology has been reviewed [2,3,5–9]. A collection of tunneling spectra of more than 200 chemical species published from 1966 to 1984 is available in the literature [4]. IETS has been used in the present study to investigate the adsorption state of anthraquinone-2-carboxylic acid (AQ-2-COOH) on oxidized Al films.

Plasma oxidation of Al produces a dense self-limiting growth oxide film that is chemically similar to alumina used in industry [10–14]. Surface-oxidized Al has served as a model for catalytic oxides, and is much easier to characterize than conventional high surface area powders [15–18]. Oxidized Al films are useful for IETS studies, while the junction is a good model system for oxide catalysts, electronic devices, and solid state sensors, etc. Information about the adsorption states and chemical reactions of adsorbed species occurring on alumina can be obtained through analyses of the tunneling spectra. It has been found that the surface hydroxyl (OH) groups on alumina play an important role for the reactions of organic acids, esters, and amides, where the anions formed from these reactions are adsorbed on the Lewis-acid sites (Al^+) on the alumina surface [7,8]. We have also employed atomic force microscopy (AFM) to observe the surface morphology of Al films evaporated at various temperatures on mica [19–26]. The surface of the Al films prepared at room temperature under high vacuum consists of spherical grains having diameters of about 100 nm, while the Al films evaporated onto heated mica at 250–350 °C show atomically-smooth surfaces. We have used AFM and X-ray photoelectron spectroscopy (XPS) to characterize the morphology and adsorption state of tetracyanoquinodimethane (TCNQ) deposited from various solutions onto the atomically-smooth oxide surfaces of Al films [21–24].

Anthraquinone-2-carboxylic acid (AQ-2-COOH) was used as a sample molecule for studying the adsorption on alumina in the present study, because its properties and the adsorption on metal surfaces have been investigated as follows. The different crystal forms of AQ-2-COOH were determined by use of various analytical techniques and their physicochemical properties, such as solubilities, partition coefficients, and heats of solution, etc. were investigated [27]. The adsorption of AQ-2-COOH on metal surfaces has been studied by various surface analyses [28–31]. Osawa et al. [28] measured the infrared spectra of AQ-2-COOH adsorbed on Ag electrodes in a $NaClO_4$ aqueous solution by the attenuated-total-reflection (ATR) method, and concluded that AQ-2-COOH is adsorbed on the metal surfaces through the carboxylate group. Han et al. [29] investigated the adsorption of AQ-2-COOH on Ag by infrared reflection absorption spectroscopy (IRAS), quartz crystal microbalance (QCM), and AFM. They also concluded that AQ-2-COOH is adsorbed on Ag as the carboxylate anion with its two oxygen atoms bound

symmetrically to the surface. Han et al. [30] also investigated the adsorption of AQ-2-COOH on Au by experiments (IRAS, Raman, XPS, and voltammetry) and quantum mechanical calculations. Although their theoretical considerations failed in the elucidation of the higher adsorptivity of AQ-2-COOH, they reported for the first time that AQ-2-COOH is adsorbed onto Au as the anion having a symmetrical carboxylate group on the surface even without applying positive potentials. We have already published a preliminary report on the tunneling spectra of AQ-2-COOH adsorbed on alumina doped from acetone solutions [31]. In this case, the alumina was prepared on evaporated Al films at room temperature in an oxygen-dc glow discharge. The adsorption state and morphology of AQ-2-COOH on alumina surfaces have also been investigated by XPS and AFM, respectively [31]. AQ-2-COOH was adsorbed onto the alumina surfaces as a uniform film of carboxylate anions deposited from acetone solutions with concentrations of 0.01–0.02 mg/ml. AQ-2-COOH was deposited as micron-sized particles of neutral molecules deposited from an acetone solution with a concentration of 0.10 mg/ml. AQ-2-COOH is a good sample molecule for studying adsorption from submonolayer to multilayer coverage on alumina by use of XPS and AFM. The motivation for the present study is to investigate the adsorption state and morphology of AQ-2-COOH on alumina deposited from AQ-2-COOH solutions of a wide concentration range.

In the present paper, we present for the first time IRAS spectra of AQ-2-COOH on alumina deposited from acetone solutions with various concentrations. These IRAS spectra have been investigated and compared to the tunneling spectra of AQ-2-COOH on alumina under the same experimental conditions. The vibrational frequencies and mode assignments for AQ-2-COOH deposited on alumina are given with those reported on Ag [28,29] and Au [30]. The IRAS spectra, XPS spectra, and AFM images of AQ-2-COOH on alumina, deposited from acetone solutions in the wide concentration range from 0.02 to 1.00 mg/ml, are also presented. This work presents a thorough study of the adsorption state and morphology of AQ-2-COOH deposited on the surfaces of oxidized Al films prepared at room temperature.

2. Experimental

The junction preparation and measurements of tunneling spectra have previously been described in detail [7,8]. Aluminum (Mitsuwa Chemicals, >99.999%) was evaporated from a resistively heated molybdenum boat on a clean glass slide (13 mm × 37 mm × 1 mm) at room temperature (18–28 °C) to form three strips (1 mm wide) in high vacuum (10^{-3} Pa). The surfaces of the strips were oxidized in an oxygen-dc glow discharge (10 Pa, 5 mA, 20–40 s) to form oxides (alumina). About 20 μl of acetone or ethanol solutions (0.01–0.02 mg/ml) of AQ-2-COOH (Tokyo Kasei, >99.0%) was dropwise added onto the surfaces of the strips and the excess solution was spun off. The junctions were completed with an evaporated Pb (Wako Chemicals, >99.999%) cross strip (1 mm wide). The resistances of the measured junctions were in the range of 200–570 Ω. The tunneling spectra were measured at liquid helium temperature

(4.2 K) with a tunneling spectrometer as reported previously [7,8]. A 500 Hz ac modulation signal of 3–4 mV peak to peak and a slowly varying dc voltage were applied to the junction. The Al electrode was negatively biased to the Pb electrode. A typical trace time of the tunneling spectrum was 60 min with a 3 s time constant of a lock-in amplifier (NF LI-574A). The x-axis of an x–y recorder was calibrated with a standard voltage generator. The peak positions were corrected by -1 meV (-8 cm^{-1}) owing to the energy gap of the superconducting Pb electrode. The resolution and accuracy of the peak positions were 2.5 meV (20 cm^{-1}) and less than ±1 meV (±8 cm^{-1}), respectively.

Aluminum was evaporated on mica sheets (Nisshin EM Co., Ltd., 15 mm × 50 mm × 0.1 mm) under high vacuum (10^{-4} to 10^{-3} Pa) and the fresh Al surfaces were oxidized in an oxygen-dc glow discharge (10 Pa, 5 mA, 30 s). AQ-2-COOH was deposited on the alumina surfaces from acetone solutions (0.02–1.00 mg/ml) of 70 μl at room temperature (17–25 °C) and at a humidity of 40–50%. The AQ-2-COOH deposited on oxidized Al films were pumped at a reduced pressure of 10 Pa for 5 min to remove volatile materials, and the resulting films were used for the measurements of IRAS, XPS, and AFM.

The IRAS spectra of AQ-2-COOH deposited on the oxidized Al films were measured with a Perkin Elmer Spectrum One spectrometer equipped with a globar light source and a lithium tantalate detector, and also fitted with a specular reflectance accessory (VeeMax II). The measurements were carried out in a N$_2$ gas atmosphere with unpolarized light incident to the film surface at 80°. The spectra were obtained from 100 to 400 interferograms at a resolution of 4 cm^{-1}. The IRAS spectra are shown in absorbance defined as $-\log(R_s/R_r)$, where R_s and R_r are the reflectivities of the sample and clean alumina reference, respectively. The transmission IR spectra of the acid and sodium salt of AQ-2-COOH in KBr pellets were also measured.

The XPS spectra of the AQ-2-COOH deposited on the oxidized Al films were measured with a Shimadzu ESCA-1000 photoelectron spectrometer with Mg Kα (1253.6 eV) radiation. Photoelectrons emitted normal to the surface (3 mm × 10 mm) were analyzed with a data collection interval of 0.1 eV with the analyzer pass energy set at 15.75 eV. The resolution was estimated to be 1.1 eV from the peak width of the Ag 3d$_{5/2}$ line at 368.3 eV.

The AFM images (256 pixels wide) of the deposited AQ-2-COOH were taken with a Digital Instruments NanoScope III operating in contact mode in air, by use of Si$_3$N$_4$ cantilevers of 200 μm long and a force constant of 0.06 N/m. The images were automatically plane-fitted to account for sample tilt and flattened by use of the standard NanoScope III software.

3. Results

3.1. Tunneling spectra

The tunneling spectra of AQ-2-COOH on alumina doped from either an acetone (0.02 mg/ml) or ethanol (0.01 mg/ml) solution are shown along with that of the undoped alumina in Fig. 1. Although the junctions doped from AQ-2-COOH solutions with these concentrations (0.01–0.02 mg/ml) gave
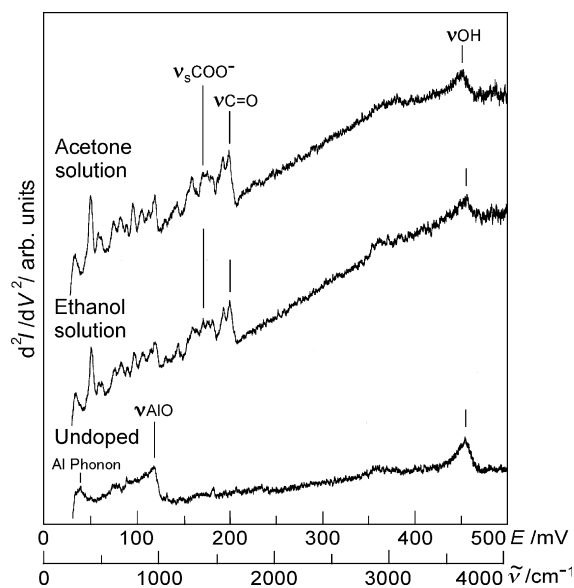

Fig. 1. Tunneling spectra of AQ-2-COOH on alumina doped from an acetone solution (0.02 mg/ml) and from an ethanol solution (0.01 mg/ml). The spectrum of undoped alumina is also shown.

good tunneling spectra, the resistances of the junctions doped from solutions with concentrations higher than 0.02 mg/ml were too large to measure the tunneling spectra. The IRAS spectrum of AQ-2-COOH on alumina obtained from an acetone solution with a concentration of 0.02 mg/ml is shown in Fig. 2a.
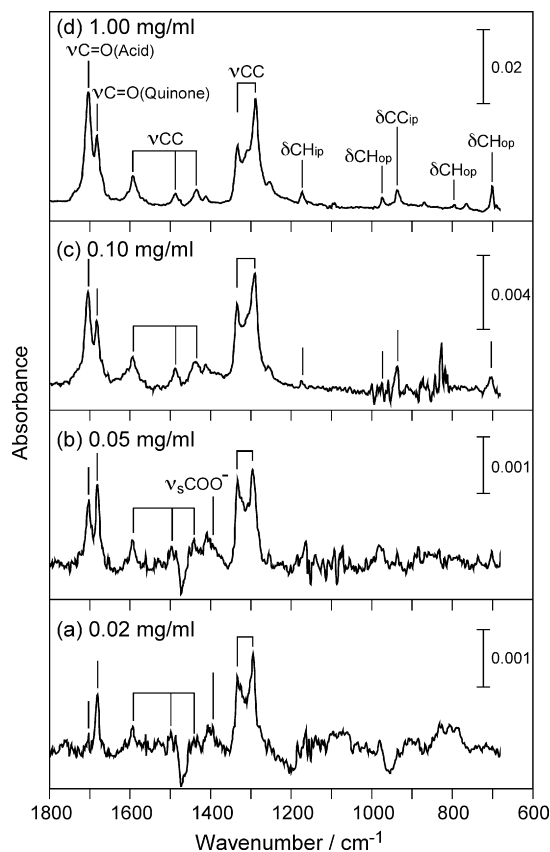

Fig. 2. IRAS spectra of AQ-2-COOH deposited on alumina from acetone solutions with concentrations of 0.02 (a), 0.05 (b), 0.10 (c) and 1.00 mg/ml (d).

Table 1
Vibrational frequencies (cm^{-1}) and mode assignments for adsorbed AQ-2-COOH on alumina deposited from acetone and ethanol solutions measured by IETS

IETS		IRAS			SERS	Assignment[a]
Acetone (6)[b]	Ethanol (3)[c]	Al[d]	Ag[a]	Au[e]	Au[e]	
3651 m br	3665 m br					νOH (surface)
3085 vw	3101 vw		3076	3076	3074	νCH
2898 w br	2919 w br					νCH (contamination)
		1701 vw				νC=O (acid)
1626 s	1625 s	1682 s	1680	1680	1666	νC=O (quinone)
1574 m	1577 m	1595 m	1593	1592	1602	νCC
1533 sh			1558			νCC
1475 m	1471 m	1488 m	1479			νCC
1440 m	1433 m	1440 m	1456			νCC
1392 m	1390 m	1398 m br	1394	1382	1383	ν_sCOO$^-$
		1330 s	1333	1333		νCC
1313 m	1309 w	1294 vs	1294	1293		νCC
1163 m	1176 m		1171		1179	δCH$_{ip}$
1059 vw	1064 vw				1088	?
					1037	?
973 m	967 m		976	975	977	δCH$_{op}$
919 w	929 vw		935	935		δCC$_{ip}$
854 m	869 m				856	?
			814			δCC$_{op}$
787 m	786 m				786	?
726 vw	728 vw					δCH$_{op}$
671 m	676 m				688	?
611 m	623 m					δCC$_{ip}$
506 m	505 m				514	?
483 m	483 m				467	?
416 vs	417 vs					?
276 m	275 m				270	?

Vibrational frequencies (cm^{-1}) and mode assignments for adsorbed AQ-2-COOH on metal films of Al, Ag, and Au measured by IRAS and on Au sol measured by SERS are also shown. Number of tunneling spectra measured and analyzed is shown in parentheses. vs, very strong; s, strong; m, medium; w, weak; vw, very weak; sh, shoulder; br, broad; ν, stretching; δ, bending or deformation; s, symmetric; ip, in-plane; op, out-of-plane.

[a] Reference [29].
[b] 0.01–0.02 mg/ml.
[c] 0.01 mg/ml.
[d] 0.02 mg/ml acetone solution.
[e] Reference [30].

The vibrational frequencies and mode assignments for the adsorbed AQ-2-COOH on alumina obtained by IETS and IRAS are shown in Table 1. The IRAS spectra had noisy spectral ranges below 1200 cm^{-1}. The values of the peak positions in the tunneling spectra and IRAS spectra are averages taken from three or six spectra measured under the experimental conditions. Although the symmetries of the infrared-active and Raman-active vibrational modes are different, the table also shows for comparison the vibrational frequencies and mode assignments for the adsorbed AQ-2-COOH on the metal films of Ag and Au measured by IRAS [29,30], and of the adsorbed AQ-2-COOH on Au sol by surface-enhanced Raman scattering (SERS) [30].

The tunneling spectrum of the undoped alumina shows medium and broad peaks of the stretching modes of the surface hydroxyl groups (νOH) and surface alumina bonds (νAlO) at about 3650 and 940 cm^{-1}, respectively [1–9]. The broadness and asymmetric tailing toward lower frequencies of the νOH

are typical features of hydrogen-bonded OH groups. The tunneling spectrum also shows the weak peak of the Al phonon mode at 304 cm^{-1} [1–9]. The very weak and broad peak observed at about 2900 cm^{-1} is due to the stretching modes of CH (νCH) attributed to hydrocarbon contamination during the junction preparation. The very weak intensity shows that the amount of contamination is negligible, and that the procedures and our apparatus for preparing tunneling junctions are appropriate. The tunneling spectra of alumina doped from acetone and ethanol were identical to that of the undoped alumina, showing that these solvents are appropriate for measuring the tunneling spectra of AQ-2-COOH on alumina.

The tunneling spectra of AQ-2-COOH show the strong peaks of the stretching modes of the quinone carbonyl groups (νC=O) at 1625–1626 cm^{-1}. However, the peak positions are shifted by 40–57 cm^{-1} to lower frequencies than those of the νC=O of AQ-2-COOH on the metal surfaces measured by IRAS and SERS. The peak shift of the νC=O peak is considered

to be due to the Coulomb interaction between an image dipole in the top Pb electrode and the dipole of the adsorbed AQ-2-COOH on the alumina surface of the junction [3,5,7]. Larger shifts of about 70 cm^{-1} were reported for νOH on the metal oxide surfaces of junctions with top Pb electrodes [3,5,7]. The tunneling spectra of AQ-2-COOH show no peaks attributed to the carboxylic acid (COOH) group. On the other hand, the spectra do show peaks corresponding to the symmetrical stretching mode of the carboxylate group (ν_sCOO$^-$) at 1390–1392 cm^{-1}, showing that AQ-2-COOH is adsorbed on the alumina surface as carboxylate anions. The peak positions of the ν_sCOO$^-$ agreed well with those of the same vibrations in the IRAS spectra on Al (1398 cm^{-1}), Ag (1394 cm^{-1}) [29], and Au (1382 cm^{-1}) [30], and that in the ATR spectrum on Ag (1392 cm^{-1}) [28]. These peak positions also agreed well with that in the SERS spectrum on Au (1383 cm^{-1}) [30]. Neither the tunneling spectra nor the vibrational spectra of AQ-2-COOH obtained by IRAS, ATR, or SERS reveal peaks corresponding to the asymmetrical stretching mode of the carboxylate group (ν_{as}COO$^-$), because of the selection rules associated with metal surfaces [1–9,28–30]. The absence of the ν_{as}COO$^-$ shows that the two oxygen atoms of the COO$^-$ group are symmetrically bonded to the metal surface [28–30]. Although the spectral range of the tunneling spectra is wider than that of the IRAS spectra, the peak positions of the vibrational modes of the CH and CC bonds in the tunneling spectra agreed well with those of the corresponding peaks in the IRAS and SERS spectra. The IRAS spectra of AQ-2-COOH on Ag and Au have peaks attributed to the in-plane and out-of-plane vibrational modes of CH and CC. This is due to a tilt of the molecular plane of AQ-2-COOH; the molecular plane is tilted by 40° and 30° from the surface normal on Ag [29] and Au [30], respectively. The peaks of the corresponding modes of CH and CC in the tunneling spectra on alumina also suggest the oblique orientation of the adsorbed AQ-2-COOH on the alumina surfaces.

Both the tunneling spectra and IRAS spectra of AQ-2-COOH on alumina show that the carboxylic acid group reacts with the OH group on the alumina surface as an acid–base reaction to give symmetrically adsorbed carboxylate anions on the Lewis-acid sites (Al$^+$) on the surface, as shown in Fig. 3 [7,8]. The very weak peak attributed to the νC=O of the carboxylic acids is present at 1701 cm^{-1} in the IRAS spectrum of AQ-2-COOH on alumina (Fig. 2a). With the exception of the νC=O for the quinone, the peak positions in the tunneling spectra and IRAS spectra of AQ-2-COO$^-$ on alumina are in good agreement. Similarly, except for the peak of the νC=O for the quinone, the tunneling spectra also agreed well with the IRAS spectra of AQ-2-COO$^-$ on Ag [28,29] and Au [30]. The

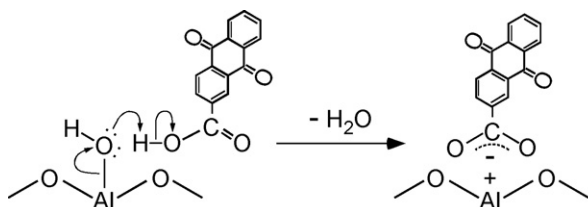absence of hydroquinone on the alumina surfaces is confirmed by the lack of peaks attributed to the νC–OH in both the tunneling spectra and IRAS spectra on alumina.

3.2. IRAS spectra

The IRAS spectra of AQ-2-COOH deposited on alumina from acetone solutions with concentrations of 0.02–1.00 mg/ml were measured and analyzed. The spectra of AQ-2-COOH deposited from the solutions with concentrations of 0.02 (a), 0.05 (b), 0.10 (c), and 1.00 mg/ml (d) are shown in Fig. 2. The spectra obtained from the solutions in the concentration range from 0.10 to 1.00 mg/ml were essentially identical. The spectra obtained from the solutions with concentrations of 0.02 (Fig. 2a) and 0.05 mg/ml (Fig. 2b) had noisy spectral ranges below 1200 cm^{-1}. They showed negative absorption features near 1470 cm^{-1} caused by the power spectra of the spectrometer. The peak positions and mode assignments of the corresponding IRAS spectra are shown in Table 2. The values of the peak positions are averages of those of three or six spectra measured under the experimental conditions. The peak positions of the transmission IR spectra of Na salt, Ag salt [29], and of the acid [29] of AQ-2-COOH (pressed in KBr pellets) are also shown in the table for comparison.

The spectrum obtained from the AQ-2-COOH solution with a concentration of 0.02 mg/ml (Fig. 2a) shows the medium and broad peak of the ν_sCOO$^-$ at 1398 cm^{-1}. The peak position agreed well with those of the transmission IR spectra of Na salt (1399 cm^{-1}) and Ag salt (1390 cm^{-1} [29]). The transmission IR spectra of both salts revealed strong peaks attributed to the ν_{as}COO$^-$ at 1605–1606 cm^{-1}, while the IRAS spectrum obtained from the same AQ-2-COOH solution with a concentration of 0.02 mg/ml showed no corresponding peak because of the selection rule on the metal surface. Although the IRAS spectrum for AQ-2-COOH on alumina exhibits a very weak peak attributed to the νC=O for acids at 1701 cm^{-1}, this peak shows that AQ-2-COOH is adsorbed on the alumina surface predominantly as carboxylate ions deposited from the solution with the same concentration. The adsorption state is consistent with that obtained from the tunneling spectra. When the concentration of the AQ-2-COOH solution is higher than 0.05 mg/ml, the peak attributed to the νC=O for the acid becomes strong, while the peak of the ν_sCOO$^-$ gradually disappears (Fig. 2b). The IRAS spectra obtained from the concentration range from 0.10 (Fig. 2c) to 1.00 mg/ml (Fig. 2d) are the same as those of the transmission IR spectra of the acid. It is considered that the alumina surface is covered with a monolayer of carboxylate anions, and the acids are present as a multilayer on the carboxylate anions.

3.3. XPS spectra

The XPS spectra of AQ-2-COOH deposited on alumina from acetone solutions with concentrations of 0.02–1.00 mg/ml were measured and analyzed. Since the alumina surface gives a very strong O 1s peak making it difficult to distinguish the corresponding peak of the adsorbed AQ-2-COOH on the

Fig. 3. Surface reaction and adsorption of AQ-2-COOH on alumina.

Table 2
Vibrational frequencies (cm^{-1}) and mode assignments for adsorbed AQ-2-COOH on alumina deposited from acetone solutions measured by IRAS

IRAS (mg/ml)			IR		IR		Assignment[a]
0.02 (3)	0.05 (3)	0.10–1.00 (6)	Na salt	Ag salt[a]	Acid	Acid[a]	
				3097	3094 vw	3092	νCH (b$_{1u}$)
	3072 vw			3078	3069 w	3068	νCH (b$_{2u}$)
				3049	3056 vw	3057	νCH (b$_{1u}$)
1701 vw	1702 s	1703 vs			1699 s	1699	νC=O (acid)
1682 s	1682 s	1682 s	1676 vs	1678	1679 vs	1678	νC=O (b$_{1u}$)
			1659 w				?
			1624 w				?
			1605 s	1606			ν_{as}COO$^-$
1595 m	1594 m	1593 m	1596 s	1593	1592 m	1592	νCC (b$_{1u}$)
			1557 m	1556	1569 sh	1569	νCC (b$_{2u}$)
1488 m	1487 m	1487 m	1485 m	1475	1487 m	1487	νCC (b$_{2u}$)
1440 m	1442 m	1436 m		1458	1434 m	1433	νCC (b$_{1u}$)
	1410 m	1412 w	1416 w		1412 m		?
1398 m br	1391 sh		1399 m	1390			ν_sCOO$^-$
1330 s	1333 s	1333 s	1334 m	1331	1332 m	1331	νCC (b$_{2u}$)
1294 vs	1295 vs	1289 vs	1293 s	1290	1282 vs	1281	νCC (b$_{2u}$)
	1256 m	1254 w	1254 w		1254 w		?
		1173 m	1172 m	1171	1172 m	1173	δCH$_{ip}$ (b$_{1u}$)
		1128 vw	1122 w		1124 vw		?
		1087 vw	1087 w		1084 vw		?
		975 m	979 w	976	974 m	972	δCH$_{op}$ (b$_{3u}$)
		937 m	938 m	935	936 m	935	δCC$_{ip}$ (b$_{2u}$)
		871 w	861 m		870 m		?
		795 vw	803 m	800	796 m	795	δCC$_{op}$ (b$_{3u}$)
			792 m				?
			766 w		766 m		?
		702 m	704 s	704	704 s	702	δCH$_{op}$ (b$_{3u}$)
			656 vw		653 vw		?
			636 vw	635	634 w	633	δCC$_{ip}$ (b$_{1u}$)

Vibrational frequencies (cm^{-1}) and mode assignments for the Na and Ag salts and acids of AQ-2-COOH in KBr pellets measured by transmission IR spectroscopy are also shown. Number of IRAS spectra measured and analyzed is shown in parentheses. vs, very strong; s, strong; m, medium; w, weak; vw, very weak; sh, shoulder; br, broad; ν, stretching; δ, bending or deformation; as, asymmetric; s, symmetric; ip, in-plane; op, out-of-plane.

[a] Ref. [29].

alumina surface, the C 1s peaks of AQ-2-COOH were used for the characterization of the adsorption state. The spectra over the C 1s region obtained from solutions with concentrations of 0.02 (a), 0.05 (b), 0.10 (c), and 1.00 mg/ml (d) are shown in Fig. 4. A linear background and a Gaussian shape with a full width at half maximum of 1.4–1.6 eV were used to deconvolute these peaks. The deconvoluted peak positions are shown with those of the spectrum of the AQ-2-COOH powder [30] in Table 3. Since the C 1 s spectrum of the AQ-2-COOH powder has been analyzed and assigned [30], the binding energies of C 1 s for the AQ-2-COOH on alumina were calibrated to the strongest peak at 284.6 eV. The values of the peak positions are averages of those obtained from four or five spectra measured under the experimental conditions. The uncertainties of the peak positions are less than ±0.1 eV.

The XPS spectra of the AQ-2-COOH deposited on alumina reveal three C 1s peaks at 284.6, 287.2, and 288.7–289.0 eV, the relative intensities of which are 81–84%, 11–13%, and 4–6%, respectively. Both the constant relative peak intensities and the widths suggest almost no contribution of organic contamination to these C 1s peaks. These three peaks are due to the C 1s of the rings (C–C), the quinone carbonyl (C=O) groups, and the carboxylate and/or carboxylic acid (COO$^-$/COOH) group of

AQ-2-COOH, respectively [30]. The peak positions (287.2 eV) of the C=O groups in the XPS spectra obtained from the solutions agreed well with that of the XPS spectrum of the AQ-2-COOH powder [30]. The peak positions (288.9–289.0 eV) of the COO$^-$/COOH group in the XPS spectra obtained from solutions with concentrations of 0.10–1.00 mg/ml (Fig. 4c and d) are very close to that (289.3 eV) of the COOH group of the neutral powder [30], although with lower binding energies. The lower binding energies are considered to correspond to the contribution of the anionic state of the AQ-2-COOH deposited on alumina [30]. The similarity in the peak positions of these spectra shows that AQ-2-COOH is deposited from these solutions predominantly in the neutral state on alumina. On the other hand, the XPS spectrum obtained from the solution with a concentration of 0.05 mg/ml (Fig. 4b) has a peak with a lower binding energy at 288.8 eV, while that obtained from the solution with a concentration of 0.02 mg/ml (Fig. 4a) has a peak at the lowest binding energy at 288.7 eV. These lower binding energies show the importance of the anionic state on the alumina surfaces. The peak position of the COO$^-$ group of the adsorbed AQ-2-COOH on Au was measured at 288.7 eV [30], showing that the AQ-2-COOH deposited on alumina from the solution with a concentration of 0.02 mg/ml is adsorbed as
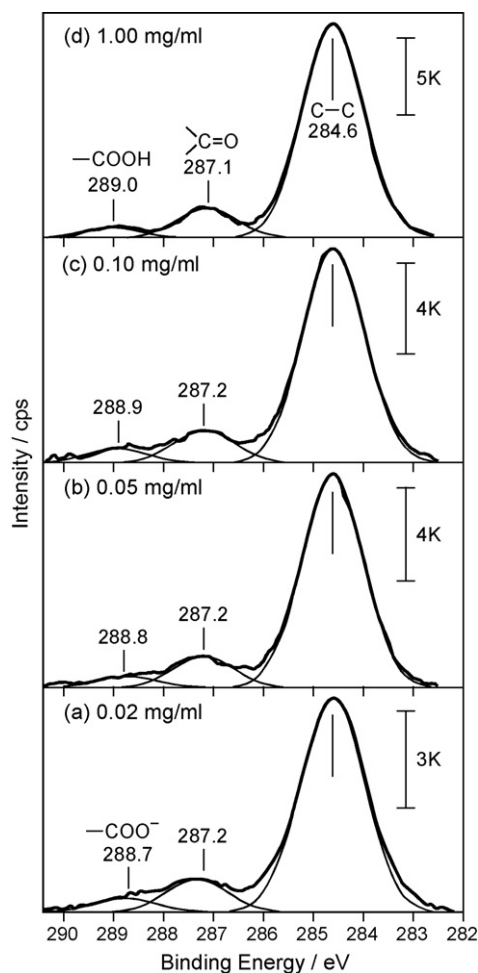
Fig. 4. XPS spectra of C 1s of AQ-2-COOH deposited on alumina from acetone solutions with concentrations of 0.02 (a), 0.05 (b), 0.10 (c) and 1.00 mg/ml (d).

carboxylate anions. The XPS spectrum of the AQ-2-COOH deposited on alumina from the solution with a concentration of 0.02 mg/ml (Fig. 4a) is consistent with the corresponding tunneling spectra and IRAS spectra. The XPS spectra of AQ-2-COOH on alumina surfaces obtained from solutions with concentrations higher than 0.02 mg/ml are also consistent with the corresponding IRAS spectra.

Table 3
C 1 s peak positions obtained from XPS spectra of AQ-2-COOH deposited on alumina from acetone solutions. C 1 s peak positions of AQ-2-COOH powder are also shown

Concentration (mg/ml)	C–C (eV)	C=O (quinone) (eV)	COO$^-$/COOH (eV)
0.02	284.6	287.2	288.7
0.05	284.6	287.2	288.8
0.10	284.6	287.2	288.9
0.20–1.00	284.6	287.1	289.0
Powder[a]	284.6	287.2	289.3

Four or five spectra obtained from the concentrations were analyzed. Uncertainties of deconvoluted peak positions are less than ±0.1 eV. Full widths at half maximum of the peaks are 1.4–1.6 eV. Relative peak intensities of the C–C, C=O, and COO$^-$/COOH are 81–84%, 11–13%, and 4–6%, respectively.

[a] Reference [30].

3.4. AFM images

The morphology of the AQ-2-COOH deposited on alumina surfaces was observed by use of AFM after the XPS measurements. The AFM observation and analysis were performed on two randomly selected places on the sample surface. Typical examples of the AFM images and their bearing histograms obtained from solutions with concentrations of 0.02 (a), 0.05 (b), 0.10 (c), and 1.00 mg/ml (d) are shown in Fig. 5. The image size is 30 μm × 30 μm wide and 100 or 200 nm gray scale. The bearing analysis provides a method of plotting and analyzing the histogram of surface heights measured over the entire sample. The surface area and volume above a certain height are calculated. Since the bearing analysis is very sensitive to the curvature of the image plane, a third-order polynomial plane fit was used to account for the sample tilt and
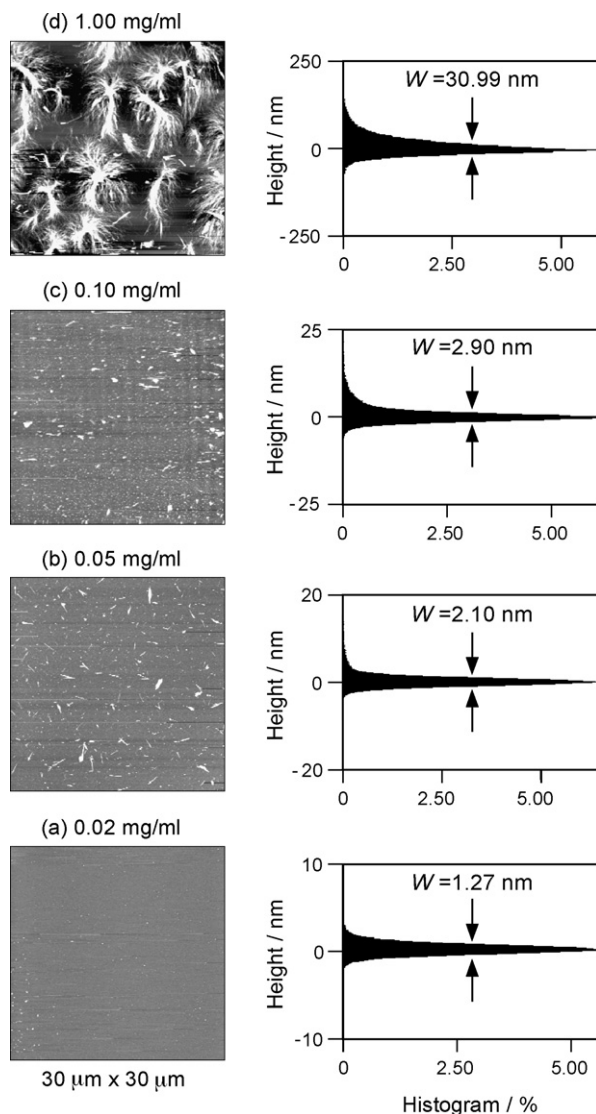

Fig. 5. AFM top views (left) and bearing histograms (right) of AQ-2-COOH deposited on alumina from acetone solutions with concentrations of 0.02 (a), 0.05 (b), 0.10 (c), and 1.00 mg/ml (d). Image size: 30 μm × 30 μm and 100 nm gray scale (0.02 (a), 0.05 (b) and 0.10 mg/ml (c)) and 200 nm gray scale (1.00 mg/ml (d)).

slight curvature. The peak in the histogram represents the surface height distribution and its width (full width at half maximum: W) is a good measure of the surface roughness [21–26]. If the surface height distributes randomly around the surface height at 0 nm, the peak has a Gaussian shape with standard deviation R_{ms}. Thus, W is represented by $2.36R_{ms}$ and most (>95%) areas of the peak are in the $2W$ region between $\pm W$ [21–26]. We have defined the bearing volume (V) as the volume in the bearing curve in the $2W$ region [21–26]. The average values of W and V of the images of AQ-2-COOH deposited on alumina are shown along with the numbers of the images observed and analyzed in Table 4. The uncertainties are standard deviations.

The AFM images of AQ-2-COOH deposited on alumina from the solution with a concentration of 0.02 mg/ml (Fig. 5a) show smooth surfaces and no particles on the surfaces. The value of W (1.27 ± 0.27 nm) of the peak in the histogram for this sample agreed well with that (1.30 ± 0.34 nm) for the undoped sample, indicating that no AQ-2-COOH particles (−0.09 ± 0.26 μm^3) were deposited on the alumina surface. The image and the bearing analysis show the presence of a very thin and uniform film of AQ-2-COOH anions on the alumina surface. This finding is consistent with those obtained for the corresponding samples by IETS, IRAS, and XPS. The values of W for the AFM images obtained from the solutions with concentrations higher than 0.02 mg/ml increase with increasing the concentration, suggesting a contribution from surface roughening and/or very small surface reaction products of the AQ-2-COOH anions. The value of W (2.21 ± 0.52 nm) for the AFM images obtained from the solution with a concentration of 0.05 mg/ml (Fig. 5b) increases about 0.9 nm by an additional monolayer of AQ-2-COOH anions on the surfaces. The increase of W is very close to the thickness (1.04–1.06 nm) of the monolayer of the adsorbed AQ-2-COOH anions on Ag obtained by ellipsometry and the IRAS data [29]. The images obtained from the solutions with concentrations higher than 0.05 mg/ml show particles on the alumina surfaces. The particles are uniformly distributed on the surfaces and their size is of the order of 1 μm in length and 10 nm in height. The heights of the deposited particles increase with increasing the concentration. It is considered from the results obtained by

IRAS and XPS that the deposited particles are neutral AQ-2-COOH molecules. The bearing histograms distribute up to 100 nm as the concentration increases to 1.00 mg/ml (Fig. 5d). The histograms of the images of the AQ-2-COOH-deposited samples from the solutions with concentrations of 0.05–1.00 mg/ml give volumes of about 1–35 μm^3 for deposited particles. The volume of the deposited particles increases slowly up to the concentration of 0.30 mg/ml and increases rapidly above this concentration.

4. Discussion

Both the surface morphology and bulk structures of the evaporated Al films on mica at various temperatures have been characterized by AFM and transmission electron diffraction and microscopy (TED/TEM) [19,20,26]. The AFM images (1 μm × 1 μm wide) of the evaporated Al films at room temperature show that the surfaces consist of round grains with diameters of about 100 nm, and have a roughness (R_{ms}) of about 2 nm. The surface morphology is mainly caused by self-shadowing during evaporation, because the surface diffusion of adatoms is too small to diffuse into the shadowed regions at these temperatures ($T/T_m = 0.32$, where T and T_m are the temperatures (K) of the mica substrate and the melting point of Al, respectively) [25,26]. The TED patterns of the Al films have the characteristic six-fold symmetry spots produced by the (1 1 1) face of a face-centered cubic (f.c.c.) lattice. The TEM micrographs also show that the films consist of grains with diameters of about 100 nm. These results show that the Al films evaporated at room temperature are microcrystalline.

Alumina surfaces have been studied by infrared spectroscopy and appropriate models proposed [15–18]. According to the surface models of the ideal planes of γ-Al$_2$O$_3$ and η-Al$_2$O$_3$ proposed by Knözinger and Ratnasamy [18], the preferentially exposed faces are the (1 1 0) faces of γ-Al$_2$O$_3$ and the (1 1 1) faces of η-Al$_2$O$_3$. Both aluminas have defect spinel lattices and the local ionic configurations of the Al^{3+} cations are identical. Since the net charge in a stable ionic structure should be equal or nearly equal to zero, OH anions are favorable to terminate these faces. Knözinger and Ratnasamy have shown that there are five types of OH groups on the (1 1 1) face and three types of OH groups on the (1 1 0) face. The surface OH groups on these faces have different net charge and relate to their different acidity and basicity. The protonic acidity of the OH groups decreases as their net charge becomes more negative, while their basicity increases simultaneously. The IR spectra of alumina surfaces show five bands in the frequency range of 3700–3800 cm^{-1}. Hydrogen bonding between adjacent OH groups perturbs the acidity and basicity and thus perturbs the frequencies of the OH groups to some extent at high OH densities [18].

Although the frequency is shifted downward by about 100 cm^{-1} because of the image dipole effect of the top Pb electrode [3,5,7], the tunneling spectrum of the undoped alumina shows the peak of the νOH at 3500–3700 cm^{-1}. The broadness and asymmetric tailing toward lower frequencies in the peak shape suggest that more than one type of surface OH

Table 4

Bearing widths (W) and volumes (V) obtained from the AFM images (30 μm × 30 μm wide) of AQ-2-COOH particles deposited on alumina from acetone solutions

Concentration (mg/ml) (number of images)	W (nm)	V (μm^3)
0.02 (10)	1.27 ± 0.27	−0.09 ± 0.26
0.05 (10)	2.21 ± 0.52	1.25 ± 0.45
0.10 (8)	3.97 ± 2.50	3.62 ± 3.36
0.20 (2)	3.18 ± 0.01	2.74 ± 0.16
0.30 (2)	4.94 ± 0.59	5.82 ± 0.86
0.50 (2)	24.29 ± 3.46	28.93 ± 2.96
0.70 (2)	30.22 ± 1.45	34.64 ± 0.72
1.00 (2)	34.52 ± 4.99	36.25 ± 2.48

The values of W and V for undoped alumina are 1.30 ± 0.34 nm and 1.28 ± 0.34 μm^3, respectively. Uncertainties are standard deviations.

group exists on the alumina surface, and these interact with each other through hydrogen bonding. The OH groups on alumina react with acids as solid bases. IETS has shown that carboxylic acids react with the surface OH groups of alumina to give the adsorbed carboxylate anions on the Lewis-acid sites (Al$^+$) of the surfaces [7,8]. It is clarified in the present study that AQ-2-COOH deposited from solutions with concentrations lower than or equal to 0.02 mg/ml, also reacts with the surface OH groups of alumina to give monolayers of symmetrically adsorbed carboxylate anions on the surface. The corresponding IRAS and XPS spectra also showed the presence of the predominant carboxylate anions on the alumina surface and the result is consistent with that obtained by IETS.

Comparative studies on various carboxylic acids on alumina by IETS and multiple reflection absorption infrared spectroscopy (MRAIRS) have been made and have clarified their adsorption state in monolayer coverage on the surfaces [32–36]. Devdas and co-workers [33–36] have found that the tunneling spectra of aliphatic monocarboxylic and dicarboxylic acids having ketone groups on alumina show no peak attributed to the νC=O, or at least only a very weak peak. The tunneling spectra of pyruvic acid (CH$_3$(C=O)COOH) exhibit no peaks associated with the νC=O, while those of 2-ketobutyric acid (CH$_3$CH$_2$(C=O)COOH) and 4,6-dioxoheptanoic acid (CH$_3$(C=O)CH$_2$(C=O)C$_2$H$_4$COOH) exhibit only a very weak peak [33,34]. The peak intensity of the νC=O in the tunneling spectra of the dicarboxylic acids is attenuated to various degrees [35,36]. Although the attenuation of the νC=O in the tunneling spectra is attributable to an interaction of this mode with the top Pb electrode, the details of the interaction is not clear. We have measured the tunneling spectra of *p*-acetylbenzoic acid (CH$_3$(C=O)C$_6$H$_4$COOH) on alumina [37–39] and magnesia [39], and reported on the adsorption state on these surfaces. *p*-Acetylbenzoic acid is adsorbed as carboxylate anions on both oxide surfaces, and the tunneling spectra clearly showed the strong peak of the νC=O at 1663 cm^{-1}. The tunneling spectrum of *p*-acetylbenzoic acid on alumina measured by Korman et al. [40] also showed the strong peak of the νC=O at 1680 cm^{-1}. Similarly, the tunneling spectra of AQ-2-COOH also show the strong peak of the νC=O at 1625 cm^{-1}. Although the frequency of the νC=O is shifted to a lower frequency because of the image dipole effect of the Pb electrode as mentioned above, the presence of the peak in the tunneling spectra of AQ-2-COOH shows no such interaction of the C=O groups with the top Pb electrode, as noted in the case of the aliphatic carboxylic acids [33–36].

The comparison of the present results obtained by IETS, IRAS, XPS, and AFM clarifies the features of these surface analyses. Since electrons tunnel through thinner parts of the insulator in the junction, IETS is sensitive to only areas having less than or equal to monolayer coverage. Thus, IETS provides information on the submonolayer to monolayer coverage on the surface and the chemical interaction between the adsorbed species and the surface. This coverage is obtained from solutions with concentrations lower than or equal to 0.02 mg/ml. The junction resistances doped from solutions higher than 0.02 mg/ml become too large to measure the tunneling spectra

because of the multilayer coverage of AQ-2-COOH on the surfaces. On the other hand, XPS probes the material within a few tens of nanometers on the surface and IRAS probes all the material on the surface. The peak intensities in the XPS spectra increase slowly and become almost constant, while the peak intensities in the IRAS spectra increase with increasing the concentration (0.02–1.00 mg/ml). The peaks of the neutral AQ-2COOH molecules appear in the IRAS and XPS spectra deposited from solutions with concentrations higher than 0.02 mg/ml. The AFM images show the particles of the AQ-2-COOH molecules on the alumina surfaces deposited from solutions with concentrations higher than 0.02 mg/ml. The size and volume of the particles increase rapidly when deposited from solutions with concentrations higher than 0.30 mg/ml.

5. Conclusions

The surface characterization of AQ-2-COOH deposited on alumina from sample solutions over a wide concentration range by the combination of IETS, IRAS, XPS, and AFM clearly shows the adsorption state and morphology of this carboxylic acid. It was clarified that AQ-2-COOH is adsorbed on alumina as both a uniform nanometer-scale film and as micron-sized neutral particles with heights of a few tens of nanometers. When AQ-2-COOH solutions with concentrations lower than or equal to 0.02 mg/ml are deposited on alumina, the acid molecules react with the surface OH groups of alumina to give a monolayer of adsorbed carboxylate anions having two oxygen atoms symmetrically bonded to Lewis-acid sites (Al$^+$) on the surface. However, when the solution concentration is higher than 0.02 mg/ml, neutral particles of AQ-2-COOH are formed. The present comparative study clarifies the adsorption and deposition of AQ-2-COOH on the alumina surfaces in detail.

References

[1] R.C. Jaklevic, J. Lambe, Phys. Rev. Lett. 17 (1966) 1139;
    J. Lambe, R.C. Jaklevic, Phys. Rev. 165 (1968) 821.
[2] T. Wolfram (Ed.), Inelastic Electron Tunneling Spectroscopy, Springer, Berlin, 1978.
[3] P.K. Hansma (Ed.), Tunneling Spectroscopy, Plenum, New York, 1982.
[4] D.G. Walmsley, J.L. Tomlin, Prog. Surf. Sci. 18 (1985) 247.
[5] N.M.D. Brown, in: R.J.H. Clark, R.E. Hester (Eds.), Spectroscopy of Surfaces, John Wiley and Sons, New York, 1988, p. 215.
[6] J.L. Tomlin, Prog. Surf. Sci. 31 (1989) 131.
[7] M. Higo, Bunseki Kagaku 50 (2001) 637.
[8] M. Higo, S. Kamata, Anal. Sci. 18 (2002) 227.
[9] K.W. Hipps, U. Mazur, in: J.M. Chalmers, P.R. Griffiths (Eds.), Handbook of Vibrational Spectroscopy, vol. 1, John Wiley and Sons, Chichester, 2002, p. 812.
[10] P.K. Hansma, D.A. Hickson, J.A. Schwarz, J. Catal. 48 (1977) 237.
[11] W.M. Bowser, W.H. Weinberg, Surf. Sci. 64 (1977) 377.

[12] P.K. Hansma, Phys. Rep. C 30 (1977) 145.

[13] H.E. Evans, W.M. Bowser, W.H. Weinberg, Appl. Surf. Sci. 5 (1980) 258.

[14] R.M. Kroeker, P.K. Hansma, Catal. Rev. Sci. Eng. 23 (1981) 553.

[15] J.B. Peri, J. Phys. Chem. 69 (1965) 220.

[16] A.A. Tsyganenko, V.N. Filimonov, J. Mol. Struct. 19 (1973) 579.

[17] H. Knözinger, Adv. Catal. 25 (1976) 184.

[18] H. Knözinger, P. Ratnasamy, Catal. Rev. Sci. Eng. 17 (1978) 31.

[19] M. Higo, X. Lu, U. Mazur, K.W. Hipps, Chem. Lett. (1997) 709.

[20] M. Higo, X. Lu, U. Mazur, K.W. Hipps, Langmuir 13 (1997) 6176.

[21] M. Higo, X. Lu, U. Mazur, K.W. Hipps, Chem. Lett. (1999) 679.

[22] M. Higo, T. Yoshidome, Y. Ozono, Chem. Lett. (2000) 1254.

[23] M. Higo, X. Lu, U. Mazur, K.W. Hipps, Thin Solid Films 384 (2001) 90.

[24] M. Higo, T. Futagawa, M. Mitsushio, T. Yoshidome, Y. Ozono, J. Phys. Chem. B 107 (2003) 5871.

[25] M. Higo, K. Fujita, Y. Tanaka, M. Mitsushio, T. Yoshidome, Appl. Surf. Sci. 252 (2006) 5083.

[26] M. Higo, K. Fujita, M. Mitsushio, T. Yoshidome, T. Kakoi, Thin Solid Films 516 (2007) 17.

[27] S.-Y. Tsai, S.-C. Kuo, S.-Y. Lin, J. Pharm. Sci. 82 (1993) 1250.

[28] M. Osawa, K. Ataka, K. Yoshii, T. Yotsuyanagi, J. Electron Spectrosc. Relat. Phenom. 64/65 (1993) 371.

[29] S.W. Han, T.H. Ha, C.H. Kim, K. Kim, Langmuir 14 (1998) 6113.

[30] S.W. Han, S.W. Joo, T.H. Ha, Y. Kim, K. Kim, J. Phys. Chem. B 104 (2000) 11987.

[31] M. Higo, T. Miake, M. Mitsushio, T. Yoshidome, Y. Ozono, Chem. Lett. 35 (2006) 48.

[32] A.H.M. Sondag, M.C. Raas, F.J. Touwslager, Appl. Surf. Sci. 47 (1991) 205.

[33] S. Devdas, R.R. Mallik, R. Coast, P.N. Henriksen, Surf. Sci. 326 (1995) 327.

[34] S. Devdas, R.R. Mallik, Int. J. Adhes. Adhes. 20 (2000) 341.

[35] S. Devdas, R.R. Mallik, Int. J. Adhes. Adhes. 20 (2000) 349.

[36] S. Devdas, R.R. Mallik, Int. J. Adhes. Adhes. 20 (2000) 355.

[37] S. Kamata, M. Higo, Chem. Lett. (1984) 2017.

[38] M. Higo, S. Mizutaru, S. Kamata, Bull. Chem. Soc. Jpn. 58 (1985) 2960.

[39] M. Higo, S. Mizutaru, S. Kamata, Bull. Chem. Soc. Jpn. 62 (1989) 1829.

[40] C.S. Korman, J.C. Lau, A.M. Johnson, R.V. Coleman, Phys. Rev. B 19 (1979) 994.